

# Behavior and Analysis of Laterally Loaded Model Pile in Nak-dong River Fine Sand

Kim, Young - Su\*<sup>1</sup> Seo, In - Shik\*<sup>2</sup>

Kim, Byung - Tak\*<sup>3</sup> Heo, No - Young\*<sup>4</sup>

## 요 지

본 논문은 낙동강 유역의 사질토 지반에 매입되어 수평 하중을 받는 모형 강관 말뚝의 수평 거동의 결과를 관찰하였다. 본 연구의 목적은 말뚝의 수평 거동에 대한 말뚝의 근입깊이, 지반 상대밀도, 하중 재하속도, 말뚝두부의 구속조건, 그리고 지반내의 이질층의 영향에 관하여 실험적인 연구를 수행하고 이러한 영향들을 정량화 할 수 있는 실험결과를 얻었다. 또한, 수치해석 (p-y method, modified Vlasov method, Characteristic Load Method;CLM) 결과들과 비교되었다.

본 연구에서 Vlasov 해석법에 기초한 new parameter는 깊이에 비례하는 지반반력 ( $K_n D = n_m z^n$ )에 대하여 적용할 수 있도록 개발하였다. p-y해석 모델은 비선형 거동이며, 수평 하중을 받는 깊은 기초의 설계에 유효한 방법이다. Characteristic load method (CLM)이라 불리는 새로운 방법은 p-y해석법 보다 간편하며, p-y해석법에 의한 결과와 잘 일치하고 있다. CLM방법은 무차원 변수들의 관계들로부터 수평 하중을 받는 말뚝들의 비선형 거동을 특성화 하기 위하여 차원 해석을 이용하고 있다.

p-y해석법과 수정 Vlasov방법에 이용하는 지반반력 계수와 극한 지반반력들은 직접 전단시험 결과들을 역 해석하여 구하였다. 직접전단 시험에 의한 지반반력 계수와 극한 지반반력들의 수평거동 예측에 이용하기 위한 수정계수들은 각각 0.014~0.05, 0.2~0.4로 나타났다.

p-y analysis, modified Vlasov method (new  $\gamma$  parameter), CLM 에 의한 수치해석 결과들은 상대밀도가 증가할수록 실험결과들과 잘 일치하는 것으로 나타났다. 또한  $y/D = 0.2$  이하 에서 CLM 방법의 적용성이 입증되었다.

\*1 Member, Professor, Dept. of Civil Engrg., Kyungpook Nat. Univ.

\*2 Member, Associate Professor, Dept. of Civil Engrg., Kyungdong College

\*3 Member, Graduate Student, Dept. of Civil Engrg., Kyungpook Nat. Univ.

\*4 Member, Graduate Student, Dept. of Civil Engrg., Kyungpook Nat. Univ.

## ABSTRACT

This paper shows that there are the results of a series of model tests on the behavior of single steel pipe pile which is subjected to lateral load in Nak-dong River sand. The purpose of the present paper is to estimate the effect of Non-homogeneity, constraint condition of pile head, lateral load velocity, relative density, and embedded length of pile on the behavior of single pile. These effects can be quantified only by the results of model tests. Also, these are compared with the results of the numerical methods (p-y method, modified Vlasov method; new  $\gamma$  parameter, Characteristic Load Method; CLM).

In this study, a new  $\gamma$  parameter equation based on the Vlasov method was developed to calculate the modulus of subgrade reaction ( $E_s = n_{hi}z_n$ ) proportional to the depth. The p-y method of analysis is characterized by nonlinear behavior, and is an effective method of designing deep foundations subjected to lateral loads. The new method, which is called the characteristic load method (CLM), is simpler than p-y analysis, but its results closely approximates p-y analysis results. The method uses dimensional analysis to characterize the nonlinear behavior of laterally loaded piles with respect to be relationships among dimensionless variables.

The modulus of subgrade reaction used in p-y analysis and modified Vlasov method obtained from back analysis using direct shear test (DST) results. The coefficients obtained from DST and the modified ones used for the prediction of lateral behavior of ultimate soil reaction range from 0.014 to 0.05, and from 0.2 to 0.4 respectively. It is shown that the predicted numerical results by the new method (CLM), p-y analysis, and modified Vlasov method (new parameter) agree well with measured results as the relative density increases. Also, the characteristic load method established applicability on the  $Q-M_{max}$  relationship below  $y/D = 0.2$ .

*Keywords* : Laterally loaded pile, CLM, Model test, parameter, Non-homogeneity, P-y analysis, Back analysis

---

## 1. Introduction

Pile foundations of the majority of buildings and structures and when used as foundations for retaining walls, bridge abutment, piers, fenders dolphins, anchor for bulkheads, waterfront and offshore structure, and unbalanced machines will be subjected to lateral loads. The response of a pile to lateral loads and moments is a typical example of the soil-structure interaction.

The analysis of this problem is complex due to the high non-linearity of the soil stress-strain behavior. Moreover the lateral pile response is also non-linear, even for low levels of applied load. This has been shown in previous experimental studies (Budhu and Davies, 1990; Matlock, 1970; Georgiadis and Butterfield, 1982; Murchison and O'Neill, 1984; Ting, 1987; Abendroth and Greimann, 1990; Kim et al., 1997) and has led to the use of non-linear methods of analysis. Yan and Byrne (1992) studied the effect of various factors on the soil-pile interaction with p-y curves under a simulated field stress condition using the Hydraulic Gradient Similitude

(HGS) technique in fine Ottawa silica sand.

Analysis methods in which the soil around the pile is treated as an elastic continuum have been developed by Douglas and Davis (1964), Spillers and Stoll (1964), Lenci et al. (1968), Matthewson (1969), Banerjee and Davis (1978), and Poulos (1971). Douglas and Davis (1964) presented solutions for the displacement and rotation of a thin, rigid vertical plate subjected to a lateral load and moment in an elastic half space. The solutions presented by Poulos (1971) were for flexible vertical strips. Analyses of this type model the continuity of the soil around the pile and are therefore useful for examining the interaction between closely spaced piles. Determining values of soil modulus used in such analysis is not a straightforward procedure, however, because the soil modulus varies from relatively low values near the pile, where the soil is not highly stressed, to relatively high values away from the pile, where the soil is not highly stressed.

The p-y method, devised by McClell and Focht (1958), appears to be the most practically useful procedure for the design of deep foundations under lateral loading. The reaction of the soil against the pile is related to the deflection of the pile by means of nonlinear p-y curves. Because numerical analyses are employed, this method can be used to analyze conditions where the properties of the soil or the pile vary in any fashion with depth. Methods for estimating p-y curves for various types of soil and loading conditions (static, cyclic) have been developed by Matlock (1970) for soft clay, Reese et al. (1975) for stiff clay below the water table, Reese and Welch (1975) for stiff clay above the water table, Reese et al. (1974) for sand, and Sullivan et al. (1979) for a variety of conditions.

Because p-y analyses are capable of representing a wide variety of soil and loading conditions in a realistic manner, and because the results of p-y analyses have been found to be in reasonable agreement with results of field loading tests in many cases, these analyses represent the state-of-the-art for analysis of single laterally loaded piles and drilled shafts.

The characteristic load method (CLM; Evans and Duncan, 1982) closely approximate the results of nonlinear p-y analyses. It was developed by performing nonlinear p-y analyses for a wide range of free-head and fixed-head piles and drilled shafts in clay and in sand, and representing the results as relationships among dimensionless variables. The method can be used to determine pile response.

To evaluate the effectivity of embedded pile length, relative density of foundation, lateral loading velocity, constraint condition of pile-head, and layered sand soil on the lateral pile behavior, a series of model tests in Nak-dong River sand on the model piles subjected to lateral load were performed. The experimental results (bending moment, deflection, yield and ultimate lateral load, yield bending moment) compared with numerical predictions on the basis of the p-y relationships proposed by Konder (1963) of other researchers for piles in cohesionless soils.

In this study, the modified Vlasov model that is developed a unique iterative technique to determine a consistent value of the  $\gamma$  parameter on the modulus of subgrade reaction constant was modified to calculate for the modulus of subgrade reaction proportional to the depth. Also, the numerical results (p-y method, modified Vlasov method; new parameter, Characteristic

Load Method: CLM) were compared with experimental results by using laboratory apparatus.

## 2. Model Tests

The experimental program included model tests on two stainless steel pipe ( $E = 2.14 \times 10^7$  t/m<sup>2</sup>) model piles of various length embedded into the sand soils so that a soil thickness of at least six pile diameters was available below the tip to minimize the influence of model box base. The outside diameter, flexural stiffness and wall thickness of the piles are given in Table 1. Broms (1964) showed that a laterally loaded pile behaves as an infinitely stiff member when the dimensionless length factor  $\eta L$  is less than about 2.0 and as an infinitely long member when  $\eta L$  exceeds about 4.0.

Table 1. Physical properties of model piles

Dia. (mm)	Wall thickness (mm)	Embedded length (cm)	$\eta L$			Flexural stiffness ( $10^{-3}t \times m^2$ )
			$D_r = 32/8\%$	61.8%	90%	
12.0	0.25	21	1.84	1.99	2.80	3.41
12.0	0.25	51	4.48	4.83	6.81	3.41

$\eta = \sqrt{n_b/EI}$  ;  $E = 2.14 \times 10^7 t/m^2$  ;  $I =$  moment of inertia of pile cross section

$n_b =$  the coefficient of subgrade reaction at  $z = D$ , i.e.,  $1.442t/m^3$  ( $D_r = 90\%$ ),  $260t/m^3$  ( $D_r = 61.8\%$ ),  $178t/m^3$  ( $D_r = 32.8\%$ )

To minimize the effect of soil particle size on the test results, a uniformly fine dry sand having an effective grain size of  $140\mu m$  and a uniformity coefficient of 2.0 was used in the experiments. In order to maintain a reasonably uniform sand ground, the traveling spreader was used to rain the sand into model box. The sand was readied to a three kinds of relative density of 32.8(low dense), 61.8(medium dense), and 90%(high dense), respectively, in layers of about 200mm thickness using traveling spreader method, with the model pile held firmly in position as the vertical state.

For the compute of the relative density, limiting density test (ASTM standard) was performed and then maximum void ratio and minimum void ratio are found to 1.19 and 0.88, respectively. As the traveling spreader method which can control the relative density with the drop height and hole size of drop apparatus, the relationship between hole size and relative density is given in Table 2.

As the traveling spreader method, in this study, the average difference between the measured and calculated relative density is shown to  $\pm 3\%$ . In Table 2, the average dry unit weight and the angle of internal friction of the sand were determined from the volume and the weight of the box content and measured in triaxial tests, respectively. In the experimental program on the

non-homogeneous soil, model tests are used to the model foundation which has difference between above and below of half of pile length( $H/L=0.5$ ).

Table 2. Effect of drop height and hole size on the relative density

Hole size (mm)	Drop height (cm)	Unit weight ( $\text{g/cm}^3$ )	Internal friction angle( $^\circ$ )	Relative density (%)
10.0	125.0	1.40	40	90.0
18.0	125.0	1.34	35	61.8
25.0	125.0	1.28	27	32.8

The model experimental setup is shown in Fig. 1. The model box was 800mm in height and 300 by 500mm in plan, with the lager dimension in the pile loading direction. Lateral loads were applied to an aluminum pile cap through a steel cylinder pushed by a electric motor. The applied load is measured by a 200N capacity load cell. Pile deflections were measured at two different levels along the length of the pile above the soil surface.

These deflections were used to compute the pile rotation and lateral deflection at ground level, taking into account the applied load and the flexural stiffness of the pile. Each of the piles was instrumented along the surface of pile with eight strain gauges, to provide the variation of the bending moments along the pile length. The depths at which the strain gauges were placed are shown in the bending moment diagrams.

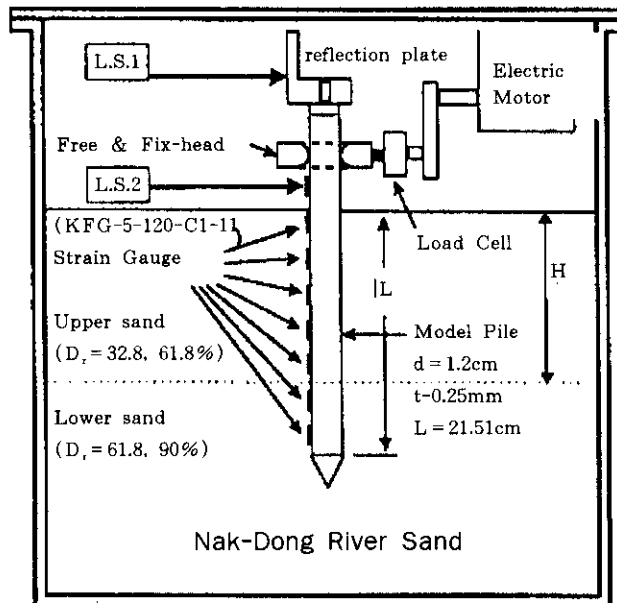


Fig.1 Schematic of the test setup

### 3. Model Test Results

Mayne and Kulhawy (1991) and Mayne et al. (1995) proposed the lateral load ( $Q$ ) - pile deflection ( $y$ ) relationship to hyperbolic function in the case of the rigid pile. But, in Nak-dong river sand, the  $Q$ - $y$  relationship is shown to second polynomial function (up to  $R^2=0.9$ ) which agree with model test results better than hyperbolic function, as shown in Fig. 2. For a deflection before the ultimate lateral load, the difference of lateral load between second polynomial function and hyperbolic function is few and the ultimate lateral load from model tests, in the case of  $D_r=90\%$ , is 2.2 times larger than the hyperbolic function suggested by Mayne and Kulhawy (1991) and Mayne et al. (1995).

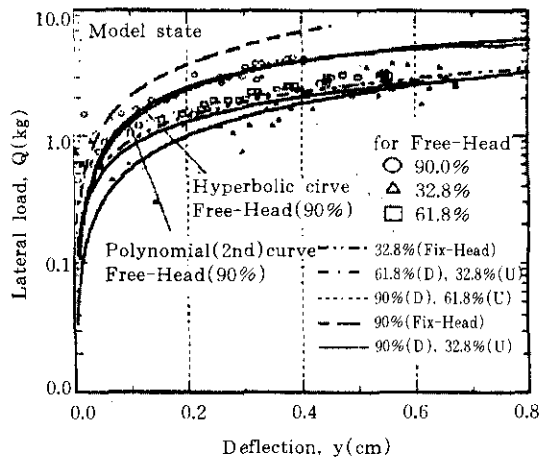


Fig.2  $Q$ - $y$  relationship under model tests

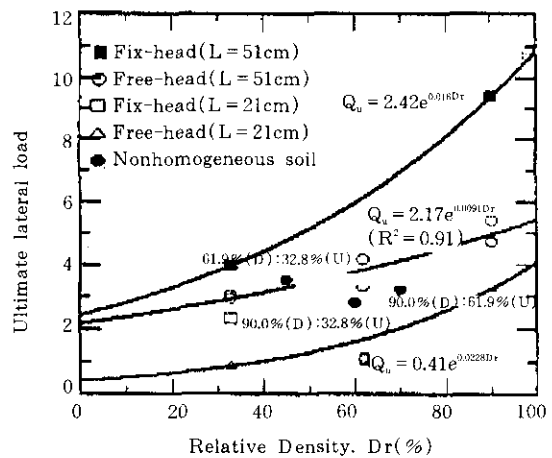


Fig.3 Relationship between relative density and ultimate lateral load for fix and free-head, nonhomogeneous soil, and  $L/D=17.5, 42.5$

Figure 3 shows the effects of relative density, non-homogeneous soil, embedded pile length, and constraint condition of pile on the ultimate lateral load. In the case of  $L/D=42.5$ , the effect of constraint condition increases more at high dense than at low dense.

From the model test results, the experimental equation for the ultimate lateral load is fitted to exponential function as follows

$$Q_u = a e^{b D_r} \quad (1)$$

where  $D_r$  is relative density and  $a, b$  are constants which have, respectively, the range of 0.41-2.42 and 0.009-0.023 for this study.

A comparison between measured ultimate lateral load and predicted one from Broms is shown in Fig. 4. It is shown that, in the case of  $L/D=42.5$ , the predicted result is 2.13 times larger than the measured ones and, in the case of  $L/D=17.5$ , about half the measured ones. At

shallow depths (less than about 5m) the API subgrade modulus,  $K_h$ , is close to the maximum soil Young's modulus,  $E_{max}$ . At greater depths, however, the  $K_h$  value becomes larger than the  $E_{max}$  value because it is specified to increase linearly with depth (Yan and Byrne, 1992).

Thus, in practice, the distribution of subgrade reaction of the field is different from the proposed one at a depth and then the ratio of predicted  $Q_u$  to measured  $Q_u$  of short piles has a reciprocal relationship with that of long piles.

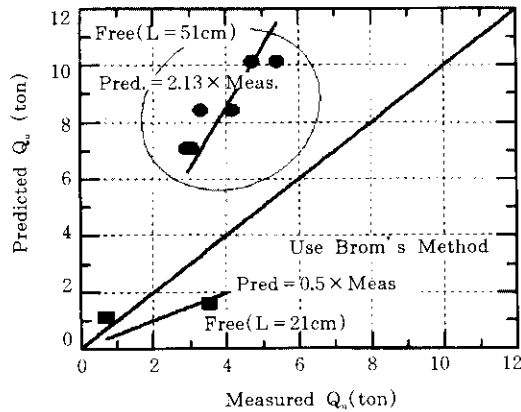


Fig.4 Comparing of measured and predicted results from Broms for ultimate load

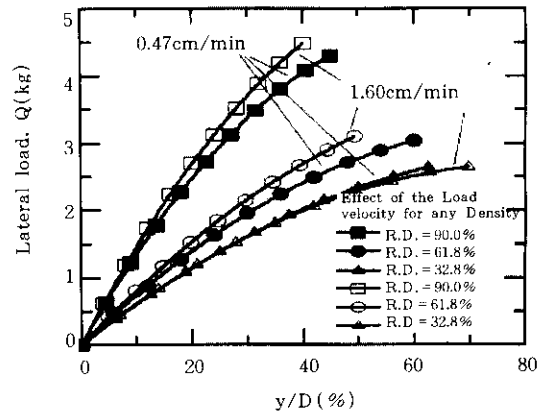


Fig.5 Q-y/d relationship under different relative density and loading velocity

### 3. 1 Relative Density and Loading Velocity Effects

Typical results of pile response and pile bending moment distribution under different relative density and loading velocity are shown in Figs. 5 and 6, respectively. These figures illustrate the influence of relative stiffness between soil and pile on the lateral pile response to monotonic pile head loading.

It can be seen that the larger the relative density and the higher the loading velocity, the stiffer the pile response. And the relationship between lateral load ( $Q$ ) and normalized deflection ( $y/D$ ) is linearity. But at the low dense ( $D_r = 32.8\%$ ) the pile response ( $Q$ - $y/D$  relationship) for loading velocity of 0.47cm/min is close to that for 1.6cm/min. Therefore, the effect of loading velocity is few for low dense of sands. The lateral loading velocity does not affect the depth of maximum bending moment .

The smaller the relative density, the deeper the depth of maximum bending moment. And the depth of maximum bending moment moves to the pile tip from 9 to 13 times pile diameter because it is specified to decrease the fixity effect of the pile tip by decrease of subgrade reaction near pile tip. Figures 6 and 7 show, respectively, the effect of relative density on the lateral load and maximum bending moment at  $y/D = 5, 10\%$ .

It appears from Figs. 6 and 7 that the larger the deflection ratio ( $y/D$ ), the larger the effect of relative density on the lateral load and maximum bending moment.

In this paper, for the conditions of free-head and  $L/D = 42.5$ , the lateral load ( $Q$ ) at a deflection, yield lateral load ( $Q_y$ ), maximum bending moment at the yield lateral load ( $MBM_y$ ), and maximum bending moment at a deflection ( $MBM$ ) are fitted to exponential function including relative density and deflection ratio. These can be expressed as

$$Q = \left( 0.03421 \frac{Y}{d} \right) \times \text{EXP} \left[ 0.0148 \times \text{EXP} \left( -0.0025 \frac{Y}{d} \right) D_r \right] \quad (2)$$

$$Q_y = 1.1085 \times \text{EXP}[0.0062 D_r] \quad (3)$$

$$MBM = \left( 0.593 \frac{Y}{d} \right) \times \text{EXP} \left[ \left( 0.012 - 8.96 \times 10^{-6} \log \frac{Y}{d} \right) D_r \right] \quad (4)$$

$$MBM_y = 22.791 \times \text{EXP}[0.0017 D_r] \quad (5)$$

where,  $y$  is deflection of pile head and  $d$  is diameter of pile and  $D_r$  is relative density of sand.

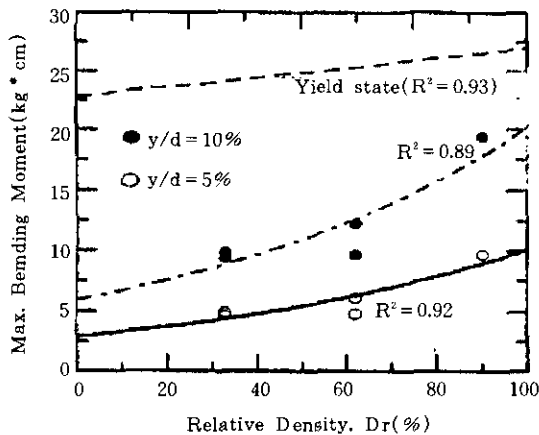


Fig.6 Relative density-Max. bending moment relationship

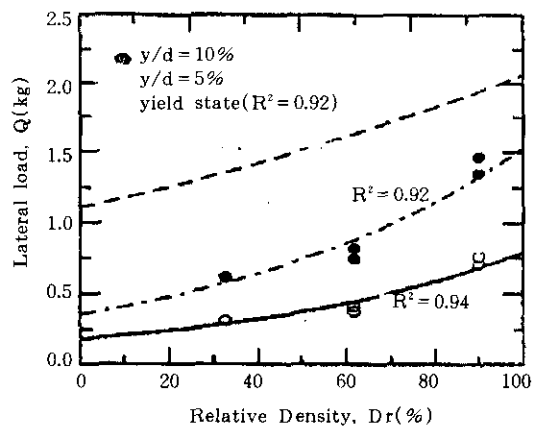
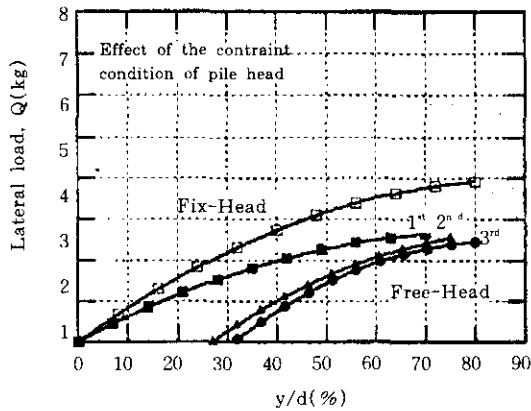


Fig.7 Effect of relative density on lateral load

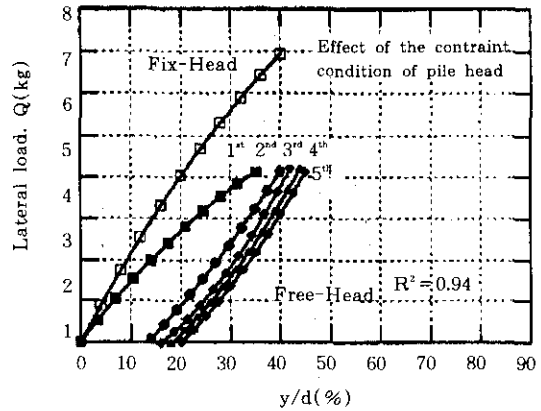
### 3.2 Pile Head Fixity Effects

Most field load tests are conducted in a free-head condition. In practice, however, few piles are connected to the superstructure in a free-head condition and some constraints are always present. Although many theoretical studies have shown that pile head fixity has a significant effect on pile response, little experimental data are available to quantify this effect, especially regarding the soil-pile interaction. Herein, the results of this model study are presented to evaluate the pile head fixity effects on pile response.





(a) for  $D_1 = 32.8\%$



(a) for  $D_1 = 90\%$

Fig.8 Q - y/D relationship for  $L/D = 42.5$

Figure 8 compares the pile responses of low and high dense under free-head and fix-head conditions. The pile response for a fix-head appears more linear and the deflection is about half of that for the free-head condition (Yan and Byrne, 1992). Similarly, for Nak-dong river sand, it is shown from Fig. 9 that the pile response for fix-head appears non-linear for  $D_1 = 32.8\%$  and linear for  $D_1 = 90\%$ . Also, the deflection for  $Q = 2\text{kg}$  is about 0.66 times of that for the free-head condition. The lateral load at the large deflection (up to  $y/d = 30\%$ ) has about the range of 1.34-1.75 times of that for the free-head condition.

Table 3 compares the bending moment distributions of low and high dense under free-head and fix-head conditions. At a deflection ( $y/D = 5\%$ ), the maximum bending moment for fix-head condition is 0.81 (at  $D_1 = 32.8\%$ ) and 0.83 (at  $D_1 = 90\%$ ) times of that for free-head condition.

By Yan and Byrne (1992), for a given applied load the fixed head reduces the peak positive bending moment below the ground to about half of that for the free head condition.

It is shown from Table 3 that the bending moment for unloading ( $y/D = 0\%$ ) state is close to that for loading state below the depth of  $21.6D$  (at  $D_1 = 90\%$ ) and  $26.2D$  (at  $D_1 = 32.8\%$ ) because of the collapse of foundation as the loading and unloading are performed. Also, at the depth of from  $10D$  to  $17.9D$ , for the fix head condition under unloading state the bending moment changes from negative moment to positive moment and it can be illustrated that the depth of foundation collapse is the range of from  $10D$  to  $17.9D$ .

### 3.3 Embedded Pile Length Effects

Typically, for a given stiffness of pile ( $EI_p$ ) and relative density, the differentiation between rigid pile and flexural pile is caused by embedded pile length. Figure 9 shows the effect of pile

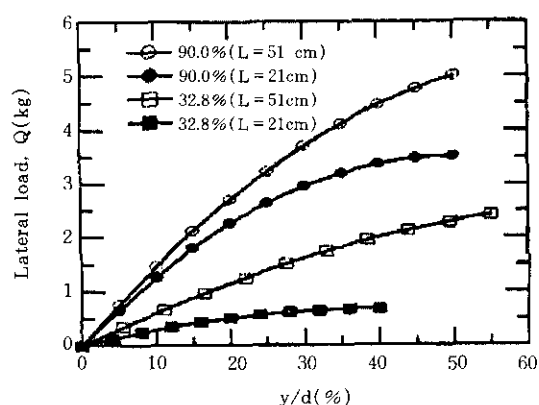
Table 3. Comparing of bending moment distribution under free-head and fix-head condition

Test code	Pile head constraint cond.	Relative Density (%)	at $y/D = 5\%$		at $y/D = 10\%$		Depth of Max. Bending Moment(cm)
			Lateral Load(kg)	Max. Bending Moment(kg × cm)	Lateral Load(kg)	Max. Bending Moment(kg × cm)	
DT2-16	Free	90.0	0.762	17.1	1.239	19.32	9.0
DT2-12	Free	61.8	0.421	12.93	0.689	15.94	9-13
DT2-26	Free	32.8	0.318	9.2	0.519	12.05	9-13
DT2-27	Free	90.0(D*)61.8(U*)	0.433	11.12	0.704	13.06	9-13
DT3-05	Free	61.8(D*)32.8(U*)	0.379	7.97	0.619	9.78	13
DT3-06	Free	90.0(D*)32.9(U*)	0.412	6.67	0.667	12.0	13
DT5-20	Fix	32.8	0.427	7.46	0.698	9.78	21.5
DT5-21	Fix	90.0	1.111	8.2	1.813	16.08	9-13

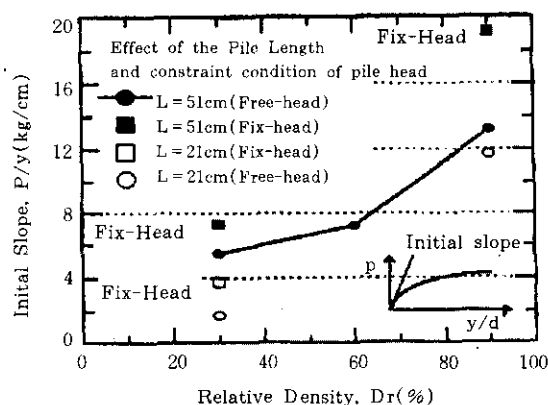
\* D and U are down and up of two layer sand, respectively.

length on the initial slope of Q-y relationship and the pile response. It is shown from Fig. 9-(a) that for  $D_r = 90\%$  the ultimate lateral load is 3.5kg at more than  $y/D = 0.45$  and for  $D_r = 32.8\%$  the ultimate lateral load is about 0.7kg at more than  $y/D = 0.35$  and there is no well defined ultimate lateral load with  $L/D = 42.5$ . Thus, the ultimate load of short pile occurs at more than  $y/D = 0.35$  and the pile response appears much more non-linear. Also, as the relative density increases from 32.8% to 90%, for the high dense the ultimate lateral load with  $L/D = 17.5$  is five times of that of low dense.

In Fig. 9-(b), it is shown that the higher the relative density( $D_r$ , 61.8%) the larger the value of initial slope of Q-y relationship. For the high dense, the effect of embedded pile length



(a) y/d-lateral load relationship for free-head



(b) Relative density-Initial slope relationship

Fig.9 Effect of pile length on the initial slope of Q-y/D relationship and pile response

on the initial slope of Q-y relationship is smaller than that for low dense. In this paper, for the conditions of long pile ( $L/D=42.5$ ), the initial slope of Q-y relationship is suggested as exponential function ( $R^2=0.93$ ) including relative density. These can be expressed as

$$(Q/y)_{\text{initial}} = 3.13e^{(0.015Dr)} \quad (6)$$

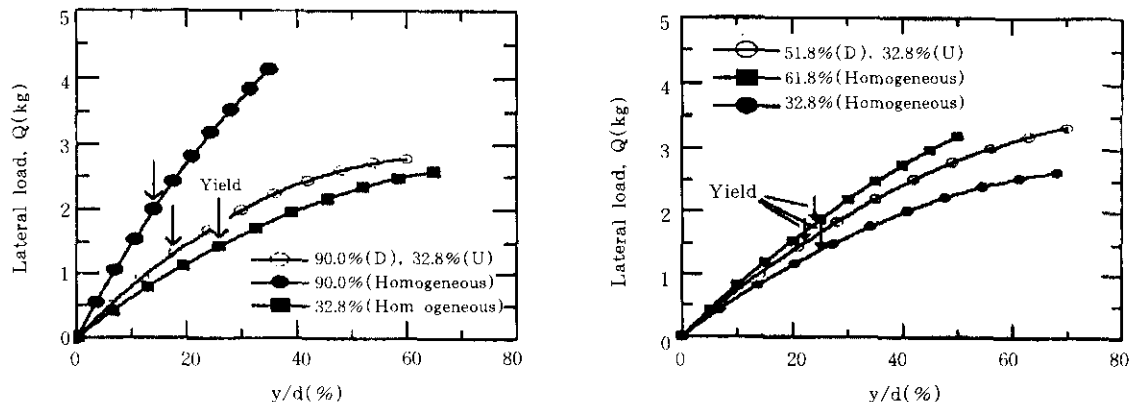
### 3.4 Non-homogeneous Effects

Most of field states are close to non-homogeneous state. However, in practice, most of model tests are performed to homogeneous soil state. In this paper, the model tests are performed to two layer ( $H/L=0.5$ ) sand soil which has different up and down on the relative densities of foundation prepared by traveling spreader method.

Figure 10 shows the effect of non-homogeneous soil on the pile response (Q-y relationship) for  $L/D=42.5$  and  $EI_p=3.41 \times 10^{-3} \text{t} \times \text{m}^2$ . Comparing of homogeneous and non-homogeneous soil for the pile response, the response is shown in the curve with second polynomial function on the homogeneous soil of upper and lower dense of layered soil and non-homogeneous soil.

In figure 10-(a), it is shown that in case of non-homogeneous soil ( $D_r=32.8\%$ : Up,  $D_r=90\%$ : Down), the response for non-homogeneous soil is close to that for homogeneous soil of upper dense rather than of lower dense. Also, the yield of lateral load is much the same as the ones of homogeneous soil of upper dense at non-homogeneous soil.

In figure 10-(b), it is shown that in case of non-homogeneous soil ( $D_r=32.8\%$ : Up,  $D_r=61.8\%$ : Down), the response for non-homogeneous soil is between that for homogeneous soil of upper dense and of lower dense. Also, the yield of lateral load, as well as in case of non-homogeneous soil ( $D_r=32.8\%$ : Up,  $D_r=90\%$ : Down), is much the same as the ones of



(a) for non-homogeneous soil ( $D_r=32.8\%$ , Up,  $D_r=90\%$ , Down)

(b) for non-homogeneous soil ( $D_r=32.8\%$ , Up,  $D_r=61.8\%$ , Down)

Fig.10 Comparing of homogeneous and non-homogeneous soil on Q-y/D relationship

homogeneous soil of upper dense at layered soil.

Consequently, for the ultimate lateral load and pile response, the larger the difference between upper and lower dense of non-homogeneous soil, the more approach the result of homogeneous soil of upper dense at layered soil.

#### 4. Numerical Analyses for Pile Response

##### 4.1 A New Parameter

A brief account of the Vlasov model is given here. The subsoil is assumed to have uniform thickness resting on a hard layer, or rock. The derivations are made for a long slab of finite width resting on an elastic foundation in plane strain conditions as shown in Fig. 11.

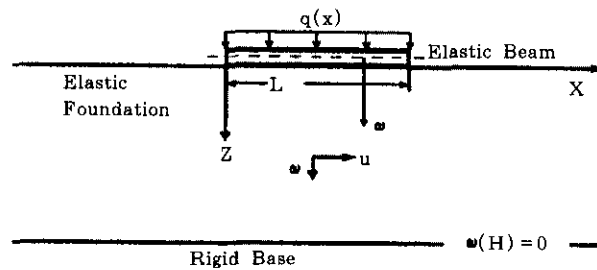


Fig.11 Beam on the elastic foundation

Using the minimum potential energy theorem, the governing equation is driven as following

$$\Pi = \int_0^L \frac{E_b I_b}{2} \left[ \frac{d^2 \bar{\omega}}{dx^2} \right] dx + \frac{b}{2} \int_{-\infty}^{\infty} \int_0^H (\sigma_x \epsilon_x + \sigma_z \epsilon_z + \tau_{xz} \gamma_{xz}) dz dx - \int_0^L q(x) \bar{\omega}(x) dx \quad (7)$$

where,  $E_b I_b$ ,  $L$ ,  $b$ , and  $H$  are flexural stiffness of the beam, length of the beam, width, and height of the soil model, respectively;  $\sigma_x$ ,  $\sigma_z$ ,  $\tau_{xz}$ ;  $\epsilon_x$ ,  $\epsilon_z$ ,  $\gamma_{xz}$  are components of stress and strains at a point in the soil, respectively.

By minimizing the function  $\Pi$  with respect to  $\omega$  and  $\phi$ , the following equation is obtained for the beam  $0 < x < L$  (Vallabhan & Das, 1991).

$$\frac{d^2}{dx^2} \left[ E_b I_b \frac{d^2 \bar{\omega}}{dx^2} \right] - 2t \frac{d^2 \bar{\omega}}{dx^2} + k \bar{\omega} = q(x) \quad (8)$$

where,

$$k = \int_0^H \frac{E_s b (1 - \nu)}{(1 + \nu)(1 - 2\nu)} \left[ \frac{d\phi}{dz} \right]^2 dz \quad 2t = \int_0^H \frac{E_s b}{2(1 + \nu)} \phi^2 dz$$

Vallabhan and Das (1988) obtained parameter  $\gamma$  by the differential equation of  $\Pi$  with respect to  $\phi$  and boundary conditions. Detailed process of these equations are presented in Vallabhan and Das (1987, 1991). Vallabhan and Das (1991) developed a new technique to determine a consistent value of the parameter on the modulus of subgrade reaction ( $E_s$ ) constant. In this study, however, this model is modified to the calculate on the modulus of subgrade reaction ( $E_s$ ) proportional to the depth. The following expression for the value of is obtained

$$\left(\frac{\gamma}{H}\right)^2 = \frac{1 - 2\nu \int_0^L \left(\frac{d\bar{\omega}}{dx}\right)^2 dx + \sqrt{\frac{k}{2t}} [\bar{\omega}^2(0) + \bar{\omega}^2(L)]}{2(1-\nu) \int_0^L \bar{\omega}^2 dx + \sqrt{\frac{2t}{k}} [\bar{\omega}^2(0) + \bar{\omega}^2(L)]} \quad \text{for } k_h = \text{const.} \quad (9)$$

$$\left(\frac{\gamma}{H}\right)^2 = \frac{1 - 2\nu \left\{ \int_0^L E_s \left(\frac{d\bar{\omega}}{dx}\right)^2 dx + n_{hi} \frac{k}{2t} \bar{\omega}^2(L) e^{2L\sqrt{\frac{k}{2t}}} \left[ \frac{\Gamma(n+1)}{\left(2\sqrt{\frac{k}{2t}}\right)^{n+1}} + \frac{e^{-2L\sqrt{\frac{k}{2t}}}}{2\sqrt{\frac{k}{2t}}} \left( L^n + \frac{nL^{n-1}}{2\sqrt{\frac{k}{2t}}} + \frac{n(n-1)L^{n-2}}{4\frac{k}{2t}} \right) \right] \right\}}{2(1-\nu) \left\{ \int_0^L E_s \bar{\omega}^2 dx + n_{hi} \bar{\omega}^2(L) e^{2L\sqrt{\frac{k}{2t}}} \left[ \frac{\Gamma(n+1)}{\left(2\sqrt{\frac{k}{2t}}\right)^{n+1}} + \frac{e^{-2L\sqrt{\frac{k}{2t}}}}{2\sqrt{\frac{k}{2t}}} \left( L^n + \frac{nL^{n-1}}{2\sqrt{\frac{k}{2t}}} + \frac{n(n-1)L^{n-2}}{4\frac{k}{2t}} \right) \right] \right\}} \quad \text{for } k_h = n_{hi} z^n / D \quad (10)$$

To predict the pile response to lateral loading, a computer program was developed, which utilizes the finite differential method, by the author and treats the pile as an elastic beam on non-linear soil springs (Kim, et al., 1997).

## 4.2 Nonlinear Analysis

Generally, the p-y criteria of Reese et al. (1974), Konder (1963), Scott (1980), Det Norske Veritas (1980), Norris (1986), and Murchison and O'Neill (1984) were used in the evaluation of the behaviors of laterally loaded pile (Georgiadis et al., 1992). The most widely employed approach for non-linear analysis appears to be the p-y approach developed by Konder (1963). The solution requires input a series of "subgrade reaction to p-y curves" for various points along the pile. The approach (p-y curve) is presented by the following hyperbolic function

$$P = \frac{y}{\frac{1}{k_h} + \frac{y}{p_u}} \quad (11)$$

where  $k_h$  is the initial stiffness of p-y curve and  $p_u$  is the ultimate soil resistance.

For piles in sand, the value of  $k_h$ , which increases proportionally with depth (Terzaghi, 1955), is presented by the following linear function

$$k_h = n_{hi} z/D \quad (12)$$

where  $z$  is the depth below ground surface and  $n_h$  is a coefficient that depends on the density of the sand.

However, comparing measured data with the results from linear function ( $k_h = n_{hi}z/D$ ) and parabolic function ( $k_h = n_{hi}z^2/D$ ), which is obtained by shear strength test, on the pile response, it is shown that the results from parabolic function agrees very well with the ones from model tests (Kim et al., 1997).

### 4.3 Characteristic Load Method (CLM)

This method (Evans and Duncan, 1982) closely approximates the results of nonlinear  $p$ - $y$  analyses. It was developed by performing nonlinear  $p$ - $y$  analyses for a wide range of free-head and fix-head piles and drilled shafts in clay and in sand, and representing the results in the form of relationships among dimensionless variables.

The use of dimensionless variables make it possible to represent a wide range of real conditions by means of a single relationship. To form these dimensionless relationships, loads are divided by a characteristic load  $P_c$ , moments are divided by a characteristic  $M_c$ , and deflections are divided by the pile width  $D$ . The characteristic load and moment that form the basis for the dimensionless relationships are given by the following expressions:

$$\text{For clay : } P_c = 7.34D^2(E_p R_1)(S_u / E_p R_1)^{0.68} \quad (13)$$

$$\text{For sand : } P_c = 1.57D^2(E_p R_1)(\gamma' D \phi K_p / E_p R_1)^{0.57} \quad (14)$$

$$\text{For clay : } M_c = 3.86D^3(E_p R_1)(S_u / E_p R_1)^{0.46} \quad (15)$$

$$\text{For sand : } M_c = 1.33D^3(E_p R_1)(\gamma' D \phi K_p / E_p R_1)^{0.40} \quad (16)$$

where,  $P_c$  = characteristic load;  $M_c$  = characteristic moment;  $D$  = pile width or diameter;  $E_p$  = pile or drilled shaft modulus of elasticity;  $R_1$  = moment of inertia ratio, i.e. ratio of moment of inertia of the pile to the moment of inertia of a solid circular cross section,  $I_p / I_{\text{circular}}$ ;  $S_u$  = undrained shear strength of clay;  $\gamma'$  = effective unit weight of sand;  $\phi'$  = effective friction angle for sand; and  $K_p$  = Rankine coefficient of passive earth pressure.

Loads applied above the ground line induce both a load and moment at the ground line, as shown in Fig. 12. Because the behavior is nonlinear, it is not sufficient merely to add the deflections caused by the load and the moment. Instead, the nonlinear effects should be taken into account by using a nonlinear superposition procedure.

The first step in the nonlinear superposition is to calculate the deflections that would be caused by the load acting alone ( $y_p$ ), and by the moment acting alone ( $y_m$ ), as shown schematically in Fig. 12-(a) and (b).

The second step is to determine a value of load that would cause the same deflection as the moment, and a value of moment that would cause the same deflection as the load (Fig. 12-c and d).

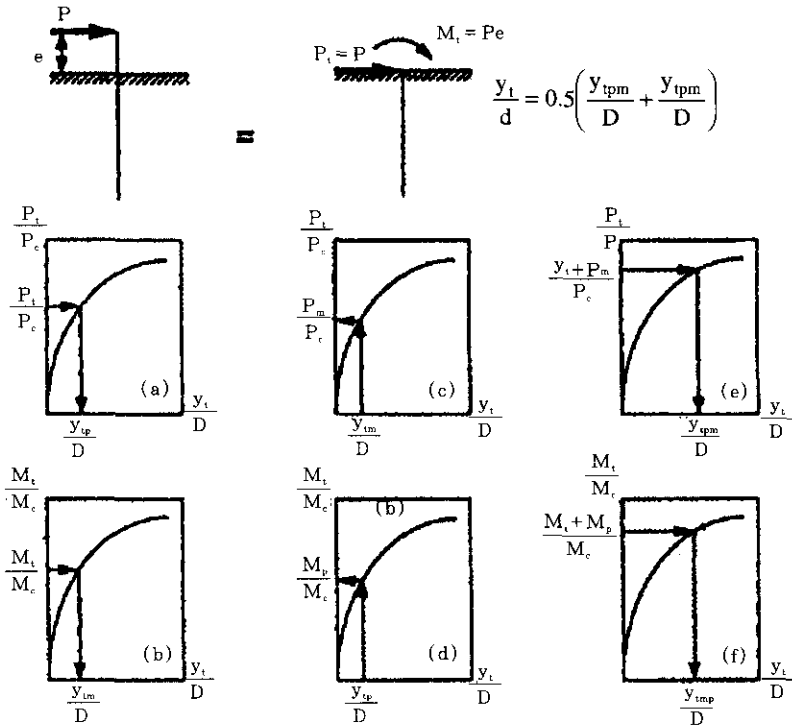


Fig.12 Nonlinear superposition of deflections due to load and moment:  
 (a)Step 1; (b)Step 2; (c)Step 3; (d)Step 4; (e)Step 5; (f) Step 6

The third step is to determine the ground line deflections that would be caused by the sum of the real load plus the equivalent load ( $P_t + P_m$ ), and the real moment plus the equivalent moment ( $M_t + M_p$ ), as shown in Fig. 12-(e) and (f).

The estimated value of deflection due to both load and moment is calculated using the equation expressed as following:

$$\text{For sand : } y_{\text{combined}} = 0.5(y_{\text{tpm}} + y_{\text{tmp}}) \quad (17)$$

where,  $y_{\text{combined}}$  = estimated ground-line deflection due to both load and moment;  $y_{\text{tpm}}$  = ground-line deflection due to the real load plus the equivalent load;  $y_{\text{tmp}}$  = ground-line deflection due to the real moment plus the equivalent.

The first step is to determine the "characteristic length, T" for the pile and soil conditions being analyzed. The value of T is determined by solving (18) for T, by repeated trial.

$$y_{\text{combined}} = \frac{2.43P_t}{E_p I_p} T^3 + \frac{1.62M_t}{E_p I_p} T^2 \quad (18)$$

where,  $T$  = characteristic length;  $y_{combined}$  = estimated ground line deflection due to both load and moment;  $y_{combined} = y_t$  if  $P_t = 0$  or  $M_t = 0$ ;  $E_p$  = pile or drilled shaft modulus of elasticity;  $I_p$  = pile or drilled shaft moment of inertia.

When the value of  $T$  has been determined, the bending moments in the upper part of the pile or drilled shaft can be calculated using the following equation:

$$M_z = A_m P_t T + B_m M_t \quad (19)$$

where,  $M_z$  = moment at depth  $z$ ;  $z$  = depth below ground line;  $A_m$  = dimensionless moment coefficient; and  $B_m$  = dimensionless moment coefficient. Values of  $A_m$  and  $B_m$  are given in Table 4.

Table 4. Moment coefficients  $A_m$  and  $B_m$  (Matlock and Reese, 1961)

Z/T	$A_m$	$B_m$
0	0.00	1.00
0.5	0.46	0.98
1.0	0.73	0.85
1.3	0.77	0.73
1.5	0.76	0.64

The principal limitation of the CLM is that it is applicable only to piles and drilled shafts that are long enough so that their behavior is not affected to any significant degree by their length. Maximum lengths necessary to satisfy this criterion depend on the relative stiffness of the pile or shaft in relation to the stiffness of the soil in which it is embedded. Minimum lengths for a number of different conditions are given in Table 5.

Table 5. Minimum pile lengths for characteristic load method

Type	Criterion	Minimum length
Clay	$E_p R_t / S_u = 100,000$	6 diameters
	$E_p R_t / S_u = 300,000$	10 diameters
	$E_p R_t / S_u = 1,000,000$	14 diameters
	$E_p R_t / S_u = 3,000,000$	18 diameters
Sand	$E_p R_t / \gamma' D \phi' K_p = 10,000$	8 diameters
	$E_p R_t / \gamma' D \phi' K_p = 40,000$	11 diameters
	$E_p R_t / \gamma' D \phi' K_p = 2,00,000$	14 diameters

## 5. Comparisons with Numerical Results

As regards the possibility of predicting the variation of the secant modulus with depth, E,



( $=k_h D$ ), the equation is rather complicated because of the influence of the different stress levels along the embedded portion of the pile. It is shown by Reese et al. (1969), Jamiolkowski (1970), and Marchetti (1977) that the secant modulus,  $E_s$ , is best approximated as following:

$$E_s = n_{hi} z^n \quad (20)$$

where,  $n$  increasing from 1 to about 2 as the pile deflection increases.

Therefore, in the paper, the secant modulus ( $E_{s(DST)}$ ) and ultimate soil resistance ( $p_{u(DST)}$ ) are determined from direct shear test (DST) for the best predicted results and are specified to increase non-linearly with depth as shown in Fig. 13. It can be expressed as following:

$$E_s = \alpha E_{s(DST)} = \alpha n_{hi} z^n \quad (21)$$

$$P_u = \beta P_{u(DST)} = \beta p_{hi} z^m \quad (22)$$

where,  $\alpha$  and  $\beta$  are modified coefficients used to predict the lateral behavior, and  $n_{hi}$ ,  $p_{hi}$ ,  $n$  and  $m$  are coefficients.

These values are summarized for each relative density and given in Table 6. The modified coefficients,  $\alpha$  and  $\beta$ , for the secant modulus and ultimate soil resistance obtained from DST obtained from back analysis for the best agreement with numerical results and the range of 0.014-0.05 and 0.2-0.4, respectively.

Table 6. The values of coefficients on relative density

$D_r$	$\alpha$	$n_{hi}$	$P_{hi}$	$\beta$	$n$	$m$
32.8	0.014	11.46	0.473	0.200	0.597	0.421
61.8	0.017	13.72	0.155	0.315	0.604	0.734
90.0	0.05	26.28	0.352	0.400	0.513	0.551

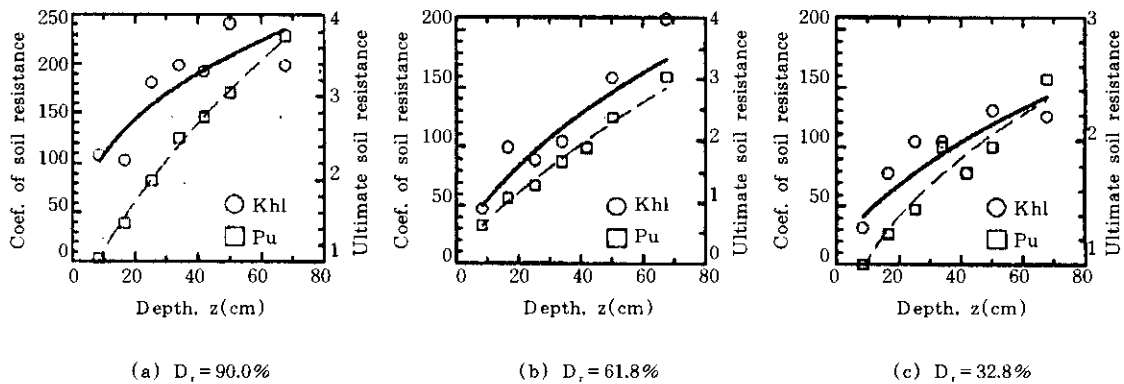
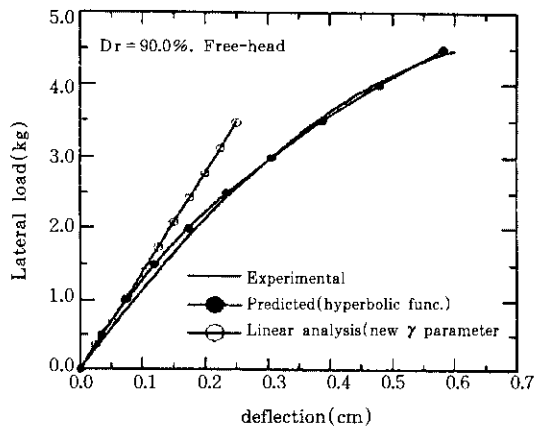


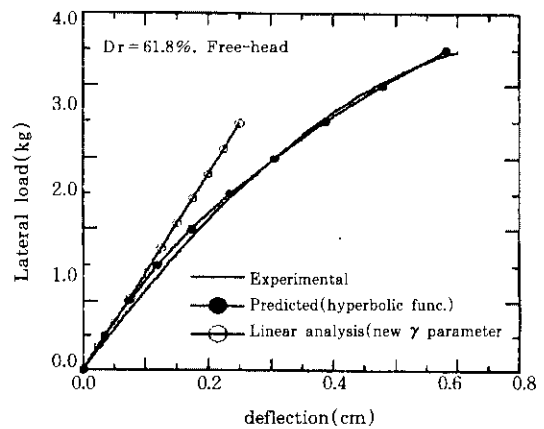
Fig.13 Change of coefficient of soil resistance( $K_h$ ) and ultimate soil resistance( $P_u$ ) with depth

Equation 21 and 22 are used to predict the pile response. The experimental and numerical predicted pile responses from  $D_r=32.8, 61.8,$  and  $90\%$ , respectively, were compared with pile responses computed using p-y curve method which is expressed as hyperbolic function and modified Vlasov method which use a new  $\gamma$  parameter.

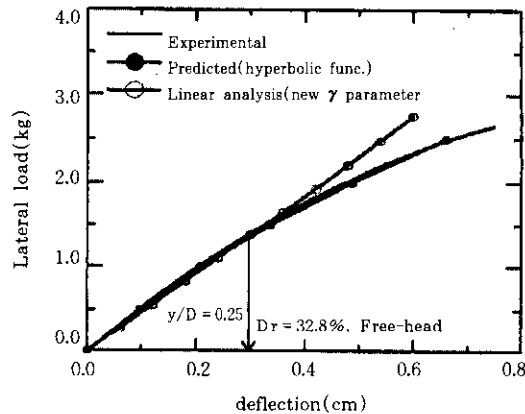
A comparison of the pile responses ( $Q$ -y relationship,  $Q$ - $M_{max}$  relationship) for  $L/D = 42.5$  and free condition at both the top and tip of pile is presented in Figs. 14 and 15, respectively. It can be shown from Fig. 14 that the predicted results from nonlinear analysis (p-y curve; hyperbolic function) and new  $\gamma$  parameter for the modulus of subgrade reaction proportional to the depth are in good agreement with measured results. Especially, the predicted result of



(a) for  $D_r=90\%$  and Free-head pile



(a) for  $D_r=61.8\%$  and Free-head pile

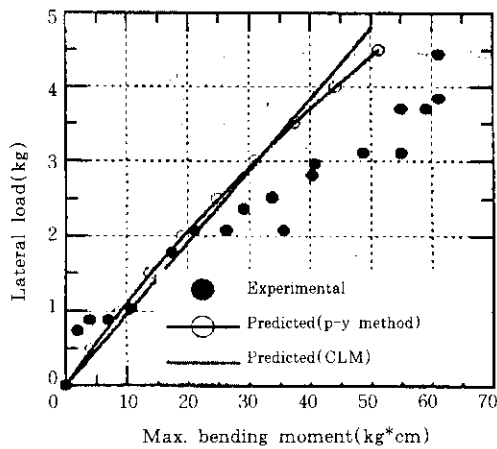


(c) for  $D_r=32.8\%$  and Free-head pile

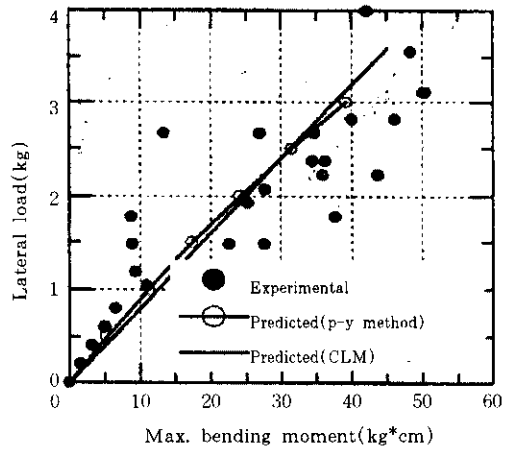
Fig.14 Comparing of measured and predicted results from p-y method and modified Vlasov method on pile response ( $Q$ -y relationship)

modified Vlasov method by new  $\gamma$  parameter is very good agreement with measured results within elastic zone ( $y/D=5\%$ ;  $D_r=90\%$ ) because this method is based on the linear stress - strain relationship. But, in the case of  $D_r=32.8\%$ , the predicted result is over-estimated below  $y/D=0.25$ .

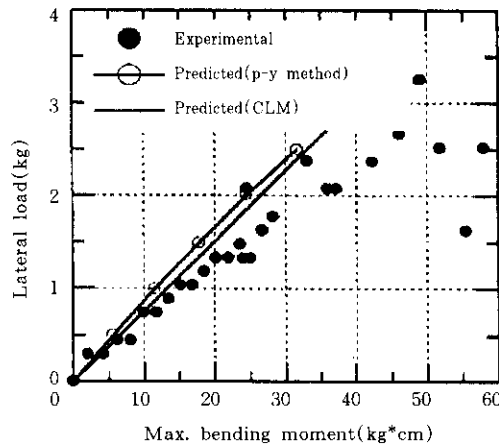
It can be shown from Fig. 15 that the predicted results from nonlinear analysis and CLM on the  $Q-M_{max}$  relationship show agreement with measured results as the relative density increases. In the case of  $D_r=90\%$ , within  $y/D=0.13$ , the predicted results of both p-y analysis and CLM are very good agreement with measured result. But, in the case of  $D_r=32.8\%$ , the predicted  $Q-M_{max}$  relationship is under-estimated beyond  $y/D=0.15$ . In the paper, the secant



(a) for  $D_r=90.0\%$  and Free-head



(b) for  $D_r=61.8\%$  and Free-head



(c) for  $D_r=32.8\%$  and Free-head pile

Fig.15 Comparing of measured and predicted results from CLM and p-y method on pile response ( $Q-M_{max}$  relationship)

modulus ( $E_{s(DST)}$ ) and ultimate soil resistance ( $p_{u(DST)}$ ) are determined from direct shear test (DST) and these values are used for the evaluation of load - deflection relationship. However, these values are obtained from soil - soil relationship, but, in practice, the p-y curve depend on the pile - soil interaction relationship. By the reason, the load - deflection relationship is very good agreement with measured result, but the difference of predicted and measured results occur as the  $y/D$  increases.

Thus, the predicted pile responses by numerical analyses (p-y analysis, modified Vlasov, and CLM) show good agreement with measured results as the relative density increases. The characteristic load method established applicability on the Q-Mmax relationship below  $y/D = 0.2$

## 6. Conclusions

Using laboratory apparatus, a series of tests were performed on single instrument model piles embedded in a Nak-dong river fine sand undergoing lateral movement. Lateral load tests were performed to evaluate the effects of constraint condition of head, pile geometry ( $L/D = 17.5 - 42.5$ ), ground condition ( $D_r = 32.8-90\%$ ), and one-way cyclic loading on lateral load-deflection response of steel piles.

Based on these test results, the following can be concluded regarding the lateral response of rigid and flexural piles in intact fine Nak-dong river fine sand and measured results and numerical results (p-y analysis, modified Vlasov, and CLM) were compared on the pile response:

1. The lateral load - deflection relationships are linear as the relative density increases, but it can be represented by second polynomial function.
2. Ultimate lateral capacity can be represented adequately by parabolic function including the relative density. Comparing measured and predicted (Broms theory) value of the ultimate lateral load, the ratio predicted lateral load to measured one will have the range from 0.5 to 2.13 for  $EI = 33,460 \text{ kg} \times \text{cm}^2$ , free-head, and free-tip conditions.
3. The ratio of maximum bending moment for fix-head to free-head is 0.81 and 0.83 for  $D_r = 32.8\%$  and  $D_r = 90\%$ , respectively. The effect of unloading for bending moment is few below depth of 21.6-26.2 times pile diameter because of the collapse of foundation.
4. The ultimate lateral load of the short piles occurs at more than  $y/D = 0.35$  and pile response appears non-linear.
5. The pile response for non-homogeneous soil is close to that for homogeneous soil of upper density as the difference between upper and lower relative density of non-homogeneous soil increases.
6. The modified coefficients,  $\alpha$  and  $\beta$ , for the secant modulus and ultimate soil resistance obtained from DST are obtained from back analysis for the best agreement with numerical results and the range of 0.014-0.05 and 0.2-0.4, respectively
7. In the paper, for elastic theory, it is developed new parameter to predict the pile response

for the modulus of subgrade reaction proportional to the depth. The predicted pile responses by numerical analyses (p-y analysis, modified Vlasov, and CLM) show good agreement with measured results as the relative density increases. The characteristic load method established applicability on the  $Q-M_{\max}$  relationship below  $y/D = 0.2$ .

## References

1. Abendroth, R.E. and Greimann, L.F. (1990), "Pile behavior established from model tests", *ASCE*, Vol. 116, GT. 4, pp.571-588.
2. Broms, B.B. (1964), "Lateral resistance of piles in cohesionless soils", *J. Soil Mech. Found. Engrg.*, *ASCE*, Vol. 90, SM. 3, pp.123-156.
3. Budhu, M. and Davies, T.G. (1987), "Nonlinear analysis of laterally loaded piles in cohesionless soils", *Can. Geotech.*, Vol. 24, pp.289-296.
4. Douglas, D.J. and Davies, E.H. (1964), "The movement of buried footings due to moment and horizontal load and the movement of anchor plates", *Geotechnique*, London, England, 14, pp.115-132.
5. Evans, L.T. Jr., and Duncan, J.M. (1982), "Simplified analysis of laterally loaded piles", *Rep. No. UCB/GT/82-04*, Univ. of California, Berkeley, Calif.
6. Fleming et al. (1985), *Piling Engineering*, *John Wiley and Sons*, New York.
7. Georgiadis, M. and Butterfield, R. (1982), "Laterally loaded pile behavior", *ASCE*, 108(1), pp.155-165.
8. Georgiadis et al. (1992), "Centrifugal testing of laterally loaded piles in sand", *Can. Geotech.*, Vol. 29, pp.208-216.
9. Jamiolkowski, M.B. (1970), "Behavior of piles", *Proc. Of the Conf. Organized by the Institution of Civil Engineers in London*.
10. Jones, R. and Xenophontos, J. (1977), "The Vlasov foundation model", *Int. J. Mech. Sci.*, *Pergamon Press*, No. 19, pp.317-323.
11. Kim, Y.S., Seo, I.S., Kim, B.T., and Kim, K.Y (1997), "A study on the Lateral Behavior of Steel Pipe Piles Using the Modified Vlasov Model", *KCS*, Vol. 17, No. 3, pp. 249-260.
12. Kim, Y.S., Kim, B.T., Heo, N.Y., and Jung, S.G. (1997), "Model tests on the lateral behavior of steel pipe piles: in the Nak-dong river sand", *KGS*, Vol. 13, No. 5, pp.59-74.
13. Kim, Y.S., Kim B.T., Seo, I.S., and Bang, I.H.(1998) "Model tests and Analysis of Laterally Loaded Piles in Sand", 17<sup>th</sup> Int. Conf. on offshore Mech. and Arctic Eng.(OMAE), Lisboa, Portugal, Session OFT-C12, paper 98-3099.
14. Konder, R.L. (1963), "Hyperbolic stress-strain response: cohesive soils", *ASCE*, Vol. 89, No. 1, pp.115-143.
15. Lenci, C., Maurice, J., and Madignier, F. (1968), "Pieu vertical sollicite horizontalement", *Annales des Ponts et Chaussees*, VI, pp. 337-383.
16. Marchetti, S. (1977), "In situ tests by flat dilatometer", Paper subm. *For publication in Journ Geotech. Div. ASCE*.
17. Matlock, H. (1970), "Corelations for design of laterally loaded piles in soft clay", *Pro. 2n<sup>d</sup> Off. Tech. Conf.*, Houston, Texas, paper OTC 1204, pp.577-594.
18. Matthewson, C.D. (1969), "The elastic behavior of a laterally loaded pile", PhD thesis, Univ. of Canterbury, Christchurch, New Zealand.
19. McClelland, B. and Focht, J. A. Jr. (1958), "Soil modulus for laterally loaded piles", *Trans., ASCE*, Vol. 123, pp. 1049-1063.

20. Mayne, P.W. and Kulhawy, F.H. (1991), "Load-displacement behavior of laterally-load rigid drilled shafts in clay", *Piling and Deep Found., Proc. 4<sup>th</sup> Int. Conf. On Piling and Deep Found.*, Balkema, Rotterdam, Netherlands, Vol. 1, pp.409-413.
21. Mayne, P.W., Kulhawy, F.H., and Trautmann, C.H. (1995), "Laboratory modeling of laterally-loaded drilled shafts in clay", *J. of Geotech. Engrg.*, ASCE, Vol. 121, No. 12, pp.827-835.
22. Murchison, J.M. and O'Neill, M.W. (1984), Evaluation of p-y relationships in cohesionless soils. In analysis and design of pile foundations. *ASCE*, New York, pp.174-191.
23. Nogami, T. and Lam, Y.C. (1987), "Two-parameter layer model for analysis of slab on elastic foundation", *ASCE*, Vol. 113, GT. 9.
24. Poulos, H.G., Chen, L.T., and Hull, T.S. (1995), "Model tests on single piles subjected to lateral soil movement", *Soils and Foundations, JGS*, Vol. 35, No. 4, pp.85-92.
25. Reese, L.C., Cox, W.R., and Koop, F.D. (1974), "Analysis of laterally loaded piles in sand", *Proc. 6<sup>th</sup> Offshore Technol. Conf.*, Dallas, Tex., pp. 473-483.
26. Reese, L.C., Cox, W.R., and Koop, F.D. (1975), "Fields testing and analysis of laterally loaded piles in stiff clay", *Proc. 7<sup>th</sup> Offshore Technol. Conf.*, Dallas, Tex., pp. 671-690.
27. Reese, L.C. and Welch, R.C. (1975), "Lateral loading of deep foundations in stiff clay", *ASCE*, Vol. 101, GT. 7, pp. 633-649.
28. Spillers, W.R. and Stoll, R.D. (1964), "Lateral response of piles", *ASCE*, Vol. 90, GT. 6, pp.1-9.
29. Sullivan, W.R., Reese, L.C., and Fenske, C.W. (1979), "Unified method of analysis of laterally loaded piles in clay", *Proc., Conf. On Num. Methods in Offshore Piling*, London, England, No. 17.
30. Terzaghi, K. (1955), "Evaluation of coefficients of subgrade reaction", *Geotechnique*, Vol. 5, pp.297-326.
31. Ting, J.M. (1987), "Full-scale cyclic dynamic lateral pile responses", *ASCE*, Vol. 113, GT. 1, pp.30-45.
32. Vallabhan, C.V.G. and Das, Y.C. (1987), "A parametric study of beams on elastic foundations", *ASCE*, Vol. 114, GT. 12.
33. Vallabhan, C.V.G. and Das, Y.C. (1988), "An improved model for beams on elastic foundations", *Proc., 1988 ASME Pressure Vessel and Piping Conf.*, Pittsburgh.
34. Vallabhan, C.V.G. and Das, Y.C. (1991), "Modified vlasov model for beams on elastic foundation", *ASCE*, Vol. 117, GT. 6, pp.956-966.
35. Vlasov, V.Z. and Leont'ev, N.N. (1966), "Beams, plates and shells on elastic foundations", *Israel Program for Scientific Translations*, Jerusalem, Israel.
36. Yan, L. and Byrne, P.M. (1992), "Lateral pile response to monotonic pile head loading", *Can. Geotech., J.* 29, pp.955-970.

(received on Apr. 2, 1998)